

UCRL- 91830
PREPRINT

CIRCULATION COPY
SUBJECT TO RECALL
IN TWO WEEKS

RESULTS OF RECENT LARGE-SCALE NH_3
AND N_2O_4 DISPERSION EXPERIMENTS

R.P. Koopman
T.G. McRae
H.C. Goldwire, Jr.
D.L. Ermak
E.J. Kansa

This paper was prepared for submittal to
Third Symposium on Heavy Gases and Risk Assessment
Wissenschaftszentrum Bonn, West Germany
November 12-13, 1984

November 1984

Lawrence
Livermore
National
Laboratory

This is a preprint of a paper intended for publication in a journal or proceedings. Since changes may be made before publication, this preprint is made available with the understanding that it will not be cited or reproduced without the permission of the author.

DISCLAIMER

This document was prepared as an account of work sponsored by an agency of the United States Government. Neither the United States Government nor the University of California nor any of their employees, makes any warranty, express or implied, or assumes any legal liability or responsibility for the accuracy, completeness, or usefulness of any information, apparatus, product, or process disclosed, or represents that its use would not infringe privately owned rights. Reference herein to any specific commercial products, process, or service by trade name, trademark, manufacturer, or otherwise, does not necessarily constitute or imply its endorsement, recommendation, or favoring by the United States Government or the University of California. The views and opinions of authors expressed herein do not necessarily state or reflect those of the United States Government or the University of California, and shall not be used for advertising or product endorsement purposes.

RESULTS OF RECENT LARGE-SCALE NH_3 AND N_2O_4 DISPERSION EXPERIMENTS*

R.P. Koopman, T.G. McRae, H.C. Goldwire, Jr,
D.L. Ermak, and E.J. Kansa

ABSTRACT

Large-scale spill tests of ammonia (NH_3) and nitrogen tetroxide (N_2O_4) were recently performed at the Nevada Test Site (NTS). The tests were extensively instrumented, resulting in large amounts of data which can be used to quantitatively describe the observed phenomena. Preliminary results from both test series indicate that aerosols play a very important role in dense gas dispersion. The test data are ideally suited for model validation, and several example model-data comparisons are included in this paper. Gaussian model calculations are found to be inadequate even at long distances downwind. New and unexpected phenomena were observed and will be discussed.

1. INTRODUCTION

The Lawrence Livermore National Laboratory (LLNL) conducted a series of large-scale ($15\text{--}60\text{ m}^3$) NH_3 spill tests for the U.S. Coast Guard and The Fertilizer Institute and a series of large-scale ($3\text{--}5\text{ m}^3$) N_2O_4 spill tests for the U.S. Air Force during the summer/fall of 1983. The NH_3 tests, called the Desert Tortoise series, and the N_2O_4 tests, called the Eagle series, were conducted on the Frenchman Flat area of the Department of Energy's (DOE) NTS at essentially the same location at which the new DOE spill test facility is currently being built. The major purpose of both test series was to measure the atmospheric dispersion of the spilled material for simulated accidental releases under various meteorological conditions. The N_2O_4 tests had the additional goals of providing source strength measurements under varying wind conditions and of providing an opportunity to test foam vapor suppression equipment and emergency response procedures.

* Work performed under the auspices of the U.S. Department of Energy by the Lawrence Livermore National Laboratory under contract No. W-7405-ENG-48.

The two test series were conducted with one immediately following the other, using nearly the same diagnostic instrument array and many of the same instruments. This resulted in considerable cost savings for the test sponsors. Ammonia testing began on August 12, 1983 followed by a change-over to the N_2O_4 configuration in mid-September with N_2O_4 testing occurring between September 17 and November 30.

The purpose of this paper is to present preliminary results from the Desert Tortoise Series Data Report (to be published) and the Eagle Series Data Report (McRae et al., 1984). A brief description of the experiments and diagnostics is included along with the presentation of some of the important results. In addition, comparisons of measured gas concentrations, as a function of downwind distance, for selected tests in each of the two test series, are made with dispersion model predictions.

2. DESCRIPTION OF THE EXPERIMENTS

The temporary spill facility used for the NH_3 tests is shown in Fig. 1. The principal components of the facility were: two 9600 gal (36 m^3) capacity road tanker trucks modified for high flow rates, a six-inch diameter spill line with a remotely operated spill valve, flow meter, temperature transducer, an orifice plate at the end, and a high pressure N_2 tube trailer to supply drive gas to force the NH_3 out of the tanker trucks, to purge the system, and to provide actuator gas for the remote-control valves. The end of the spill pipe was fastened rigidly to the ground at about 1 m above ground level pointing downwind. The orifice plate was sized such that the NH_3 remained liquid until reaching the orifice plate, whereupon it flashed to a mixture of vapor and droplets, cooling rapidly, and entraining air.

The facility used for the N_2O_4 experiments was similar except that there was only one tanker truck, the spill line was three-inch diameter PVC, and several different configurations were used on the end of the pipe. A single-pipe configuration was used for spills into a confined area, and a multiple-exit configuration was used to simulate unconfined spills in which the spill rate equals the vaporization rate.

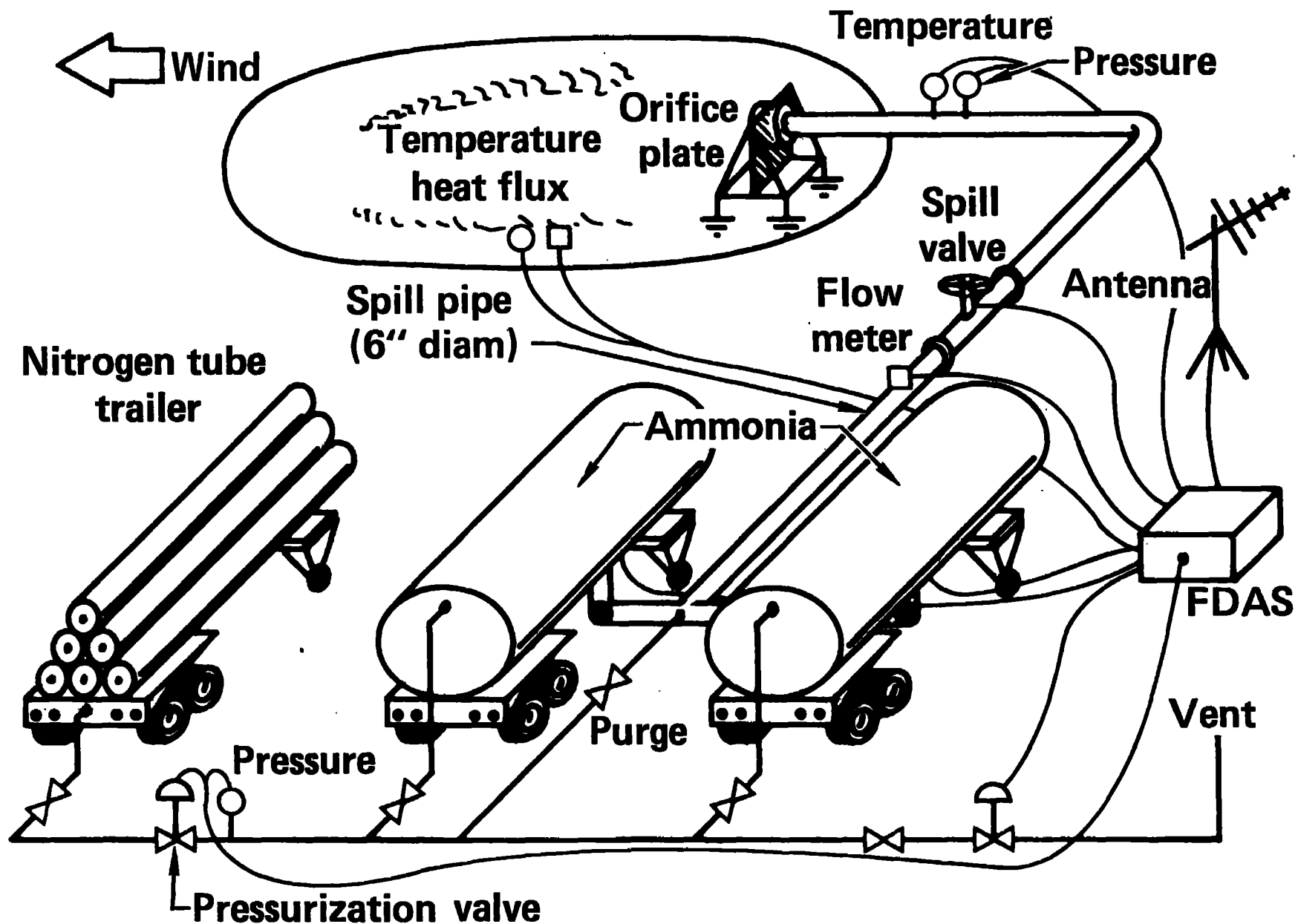


Fig. 1. Temporary ammonia spill facility used for the Desert Tortoise series of experiments at the Nevada Test Site in 1983.

A typical spill test sequence would begin with a favorable weather forecast. Then the diagnostic system would be checked for satisfactory operation, and the spill area would be cleared of all personnel except for the arming team. Members of the arming team would open the manual valve on the N_2 tube trailer, set the pressure control valve to the desired drive gas pressure and open the manual valves on the tanker trucks. The arming team would then leave the area, and all further spill operations would be conducted remotely.

When the wind speed, and stability direction, satisfied the spill criteria, the tanker trucks were pressurized and the spill was initiated. A real-time display of the volume of material spilled as a function of time was provided by the command and control data recording system (CCDRS) located about 1 km upwind. When the desired amount had been spilled, the spill was terminated. After the vapor cloud had cleared the downwind array, the pressure in the tanker trucks would be relieved and the disarming team would then enter the area and close the manual valves on the tanks to secure the facility.

Numerous measurements were made in the area of the spill. The temperature of the fluid just prior to its exit from the spill pipe was recorded. Three heat-flux sensors were placed just below the surface of the soil at different locations. For the N_2O_4 tests a thermocouple rake assembly was also installed in the spill area for the purpose of determining the temperature gradient within the liquid for the confined spills, and within the initial vapor layer of the unconfined spills. One thermocouple was at ground level, and the second and third at heights of 2 and 4 cm, respectively. Provision was also made for measuring the depth (pressure head) of the liquid N_2O_4 during the confined spills.

In addition to the spill area measurements, atmospheric boundary layer, wind field, vapor cloud temperature and concentration, and surface heat flux measurements were also made using an extensive diagnostic system developed by LLNL. There were three main arrays of diagnostic instruments: the meteorological array, the mass flux array, and the dispersion array. The locations of the various stations making up these arrays, along with the positions of the camera stations, are shown in Fig. 2.

The meteorological array consisted of eleven two-axis, cup-and-vane anemometers (all at a height of 2 m), plus a 20-m tall met. tower located

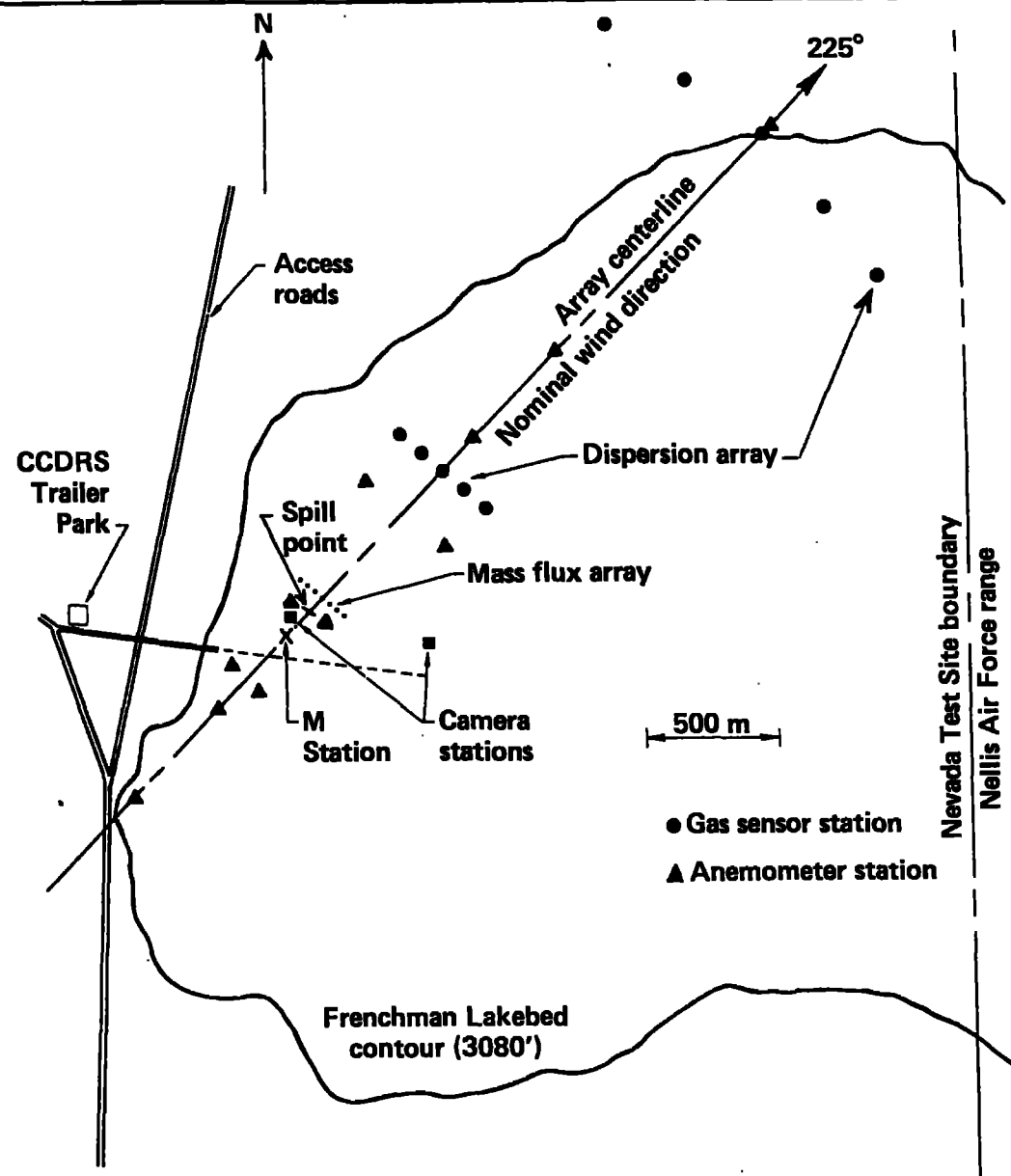


Fig. 2. Diagnostic instrument array for Desert Tortoise and Eagle series experiments.

directly upwind of the spill area. The locations of the anemometer stations are shown in Fig. 2. Wind speed and direction at each station were averaged for 10 sec, and the results, plus the standard deviation of direction for the same period, were transmitted back to the CCDRS trailer and displayed in real time. This display was the primary information used to determine the optimum time for the spill.

The meteorological tower was outfitted with four temperature gauges and three Gill bivane anemometers. This station also measured the ground heat flux. Humidity data and local barometric pressure were obtained from the NTS Weather Support Group.

A mass flux array was employed to determine the evaporation rate, or source strength. This was accomplished by measuring the gas/ aerosol concentration, vapor cloud temperature and velocity as it passed through the array. The product of the mass density and velocity integrated over the vapor cloud cross-section yields the total mass flux passing through the array at any instant. If the entire cloud is within the array, this mass flux should be equivalent to the source strength of the spilled material.

The mass flux array was located 100 m downwind of the spill area for the NH_3 tests and 25 m for the N_2O_4 tests. It consisted of seven gas stations and two anemometer stations. The centerline station was a 10 m tall tower outfitted with three bivane anemometers, plus other sensors listed in Tables I and II. The remaining six stations had 6 m tall masts and each was outfitted with instruments as indicated in Tables I and II, with the stations located at 5-m intervals to either side of the centerline station (three to each side). For the NH_3 tests, vapor concentrations were measured using MSA nondispersive IR gas sensors at 1, 3, and 6 m heights. Gas plus aerosol was passed through a heating apparatus to vaporize the aerosol and allow the total amount of NH_3 present to be determined.

A detailed description of the LLNL IR gas sensor is given in Bingham et al. (1983). The sensor produces a signal proportional to the molecular absorption of IR radiation by the N_2O_4 or NH_3 vapors as they pass through the 15 cm sample region. The sensor was calibrated by using known concentrations of N_2O_4 or NH_3 . The sensor was originally designed for the detection of liquefied natural gas (LNG) vapors and was not optimized for the detection of either NH_3 , N_2O_4 , or NO_2 . Nitrogen tetroxide rapidly dissociates into NO_2 as it mixes with air making it desirable to measure

NO₂ rather than N₂O₄. Unfortunately, sufficient funds to make these modifications were not available. Consequently, the sensors were moved close to the source (25 m) for the N₂O₄ tests.

TABLE I. DIAGNOSTIC INSTRUMENTATION USED ON THE NH₃ TESTS.

<u>Measurement</u>	<u>Instrument</u>	<u>Numbe</u>	<u>Distance from spill location</u> <u>(km)</u>				
			<u>0.0</u>	<u>0.1</u>	<u>0.8</u>	<u>2.8</u>	<u>5.5</u>
Gas concen- tration	MSA NDIR	20		x			
	LLNL IR	31		x	x		
	IST	24	x		x	x	x
	Dosimeter	8				x	x
Temperature	Thermocouple	36	x	x	x		
Aerosol density	Beta gauge	5		x			
	Nephelometer	2		x			
	Particle counter	1		x			
	LLNL IR	31		x	x		
Humidity	LLNL	1	x				
Heat flux	Hy-Cal	3		x			

TABLE II. DIAGNOSTIC INSTRUMENTATION USED ON THE N₂O₄ TESTS.

<u>Measurement</u>	<u>Instrument</u>	<u>Number</u>	<u>Distance from spill location</u> <u>(km)</u>			
			<u>0.0</u>	<u>0.025</u>	<u>0.8</u>	<u>2.8</u>
Gas concen- tration	LLNL IR	21		x		
	Interscan	2				x
	Dosimeter	8				x
	ESI	13			x	
Temperature	Thermocouple	36	x	x	x	
Aerosol density	LLNL IR	31		x	x	
Humidity	LLNL	1	x			
Heat flux	Hy-cal	3		x		

The dispersion array consisted of five 10 m towers located approximately 800 m downwind of the spill area (see Fig. 2). The purpose of this array of

sensors was to measure the downwind dispersion by recording the concentration and dimensions of the gas cloud during each spill test. All the towers had gas sensors and thermocouples located at heights of 1, 3.5, and 8.5 m above the ground. A typical data acquisition station of this type is shown in Fig. 3. The towers were separated by a distance of 100 m. In addition, there were portable ground-level stations at 2800 m, and on occasion, at 5500 m downwind. See Tables I and II for details on number of instruments and placement. Additional diagnostic instruments were also used, including cameras, and are listed in Table III.

TABLE III. ADDITIONAL INSTRUMENTATION USED ON BOTH TEST SERIES.

<u>Spill Facility Measurements</u>	<u>Weather Measurements</u>
<ul style="list-style-type: none">• Flowrate• Tank pressure• Exit pressure• Tank temperature• Exit temperature• Heat flux	<ul style="list-style-type: none">• 2-axis anemometer array of 11 stations• 3-level, 3-axis anemometers at 2 stations• Humidity• Temperature at 4 heights

Photo Documentation

- Movie cameras (4)
- Still cameras (4)
- Videotape (1)

The control of the spills and the data acquisition and storage was all performed in the CCERS trailer. This system utilizes UHF radio telemetry for command and data transmission and is designed to acquire data from sensors distributed over an area with a diameter of up to 10 miles (Baker, 1982). All of the remote data acquisition stations and sensors are battery-powered, portable, gas-tight, and ruggedized. Batteries are recharged by solar cells. This network of 24 stations acquired data from up to 285 channels at a rate of one sample per second for the gas and control stations and one sample per 10 seconds for the wind-field stations.

After each test, raw data are converted to calibrated data sets. These reduced data are written to an ASCII magnetic tape and transferred to the LLNL Computation Center for archival preservation. The data base tables are stored on an off-line mass storage system and are readily available for analysis.

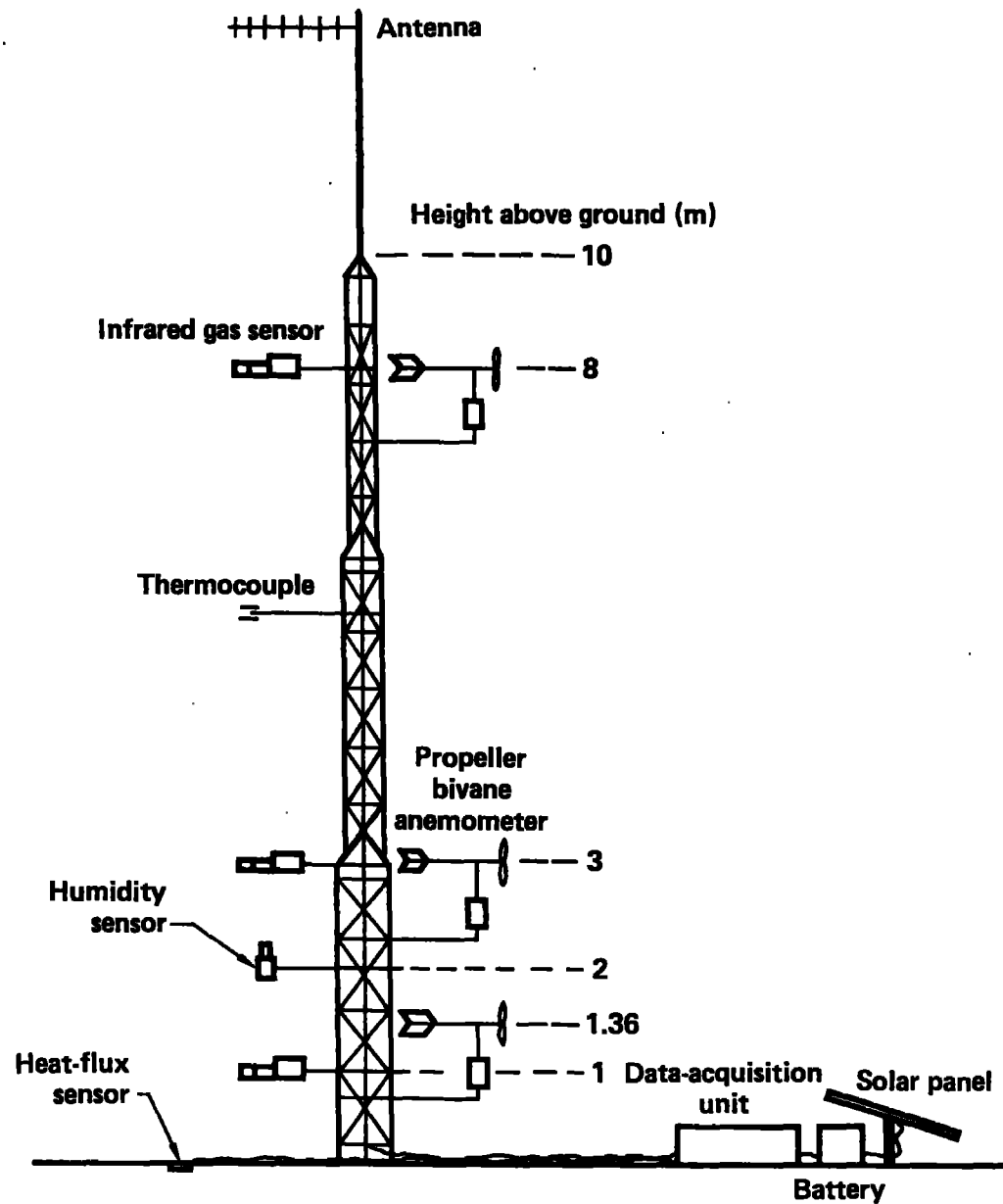


Fig. 3. A typical gas sensor station showing many of the instruments used for measurement of the dispersing gas cloud.

Test summaries, listing spill conditions and meteorological conditions, are given in Table IV and V for the two test series. Estimates of stability class came from vertical temperature gradients and horizontal wind variability σ_z .

TABLE IV. TEST SUMMARY FOR DESERT TORTOISE SERIES NH_3 SPILLS.

<u>Test</u>	<u>Date</u>	<u>Size (m^3*)</u>	<u>Rate (m^3/min)</u>	<u>Wind speed (m/s)</u>	<u>Wind direction</u>	<u>Stability class</u>
1	8/24	15	7.3	7.3	228°	C
2	8/29	43	10.3	5.6	223°	C
3	9/1	30	10.0	7.3	221°	C
4	9/6	60	8.0	4.8	224°	E

TABLE V. TEST SUMMARY FOR EAGLE SERIES N_2O_4 SPILLS.

<u>Test</u>	<u>Date</u>	<u>Size (m^3*)</u>	<u>Rate (m^3/min)</u>	<u>Wind speed (m/s)</u>	<u>Wind direction</u>	<u>Stability class</u>
1	9/17	1.3	1.75	6.2	233°	C
2	9/23	1.5	1.4	5.8	223°	A
3	10/7	4.2	1.4	3.1	229°	D
4	10/13	2.8	0.5	4.9	233°	D
5	10/16	1.3	0.6	2.2	261°	A
6	10/30	3.4	0.7	5.0	223°	D

* $1 \text{ m}^3 = 264 \text{ gallons}$

3. RESULTS

3.1 Preliminary N_2O_4 Results

The Eagle 3 test was the largest of the N_2O_4 test series with the material spilled unconfined onto the desert soil from the multiple-exit configuration. It was conducted under nearly ideal atmospheric conditions for the observation of dense gas effects on dispersion, one of the goals of the test series. The vapor cloud traveled directly down the array centerline producing NO_2 concentrations in excess of 500 ppm at 785 m. One of the portable NO_2 sensors located on the array centerline at 2800 m recorded a peak concentration of 9 ppm.

As the liquid N_2O_4 spilled, it was observed to evaporatively cool to its freezing point. The vapor temperature at a height of 2 cm and located

approximately 1 m from one of the spill points is shown in Fig. 4. The normal freezing point for N_2O_4 is $-12.2^{\circ}C$. This behavior would be expected if the N_2O_4 were allowed to pool. However, examination of the video tapes showed that very little of the N_2O_4 actually formed liquid pools. It either evaporated or was absorbed into the ground.

The ground heat flux as measured directly below the soil surface in the spill area is shown in Fig. 5. The sign convention for the ground heat flux is such that a positive value represents heat flowing into the ground. The drop in heat flux during the spill was much less than expected. Assuming that the multi-exit spill system distributed the N_2O_4 uniformly over a 20 m diameter area, and that it evaporated as fast as it was spilled, would require a total heat flux of about 50 kWatt/m^2 . We see from Fig. 5 that the peak measured ground heat flux is about 100 times less than this amount. Clearly the N_2O_4 did not evaporate as quickly as it was spilled. If one assumes a uniform heat flux of 0.50 kWatt/m^2 over the 20-m-diameter spill area, the resulting source strength is calculated to be 23 kg/min. This value (23 kg/min) is considered to be a minimum estimate of the source strength since it does not include the other sources of heat. The actual source strength would consist of the sum of the ground heat flux component, the sun and air heat addition component, and internal energy component.

It became immediately obvious upon examination of the Eagle 1 spill results that something other than N_2O_4 and/or NO_2 vapors were present in the vapor cloud. The LLNL IR sensor detects molecular absorption in four different spectral regions. For mixtures of N_2O_4 and NO_2 vapors, two spectral regions experienced absorption (signal channels) while the other two did not (reference channels). If only N_2O_4 or NO_2 vapors were to pass through the sensor absorption region, strong attenuation would be expected in the signal channels and little attenuation would be expected in the reference channels. For all of the Eagle series spills the observed attenuation in the reference channels was almost equivalent to that of the signal channels.

Prior to the Eagle 3 spill, the IR sensors were tested using N_2O_4 vapors directly from the tanker. The sensors behaved as expected, showing little attenuation in the reference channels. During the Eagle 3 spills, grab samples of the vapors were obtained as the cloud passed through the 25 m array. A grab sample of the vapors of the N_2O_4 in the spill pipe was also obtained. These grab samples were analyzed later at LLNL by both mass and IR

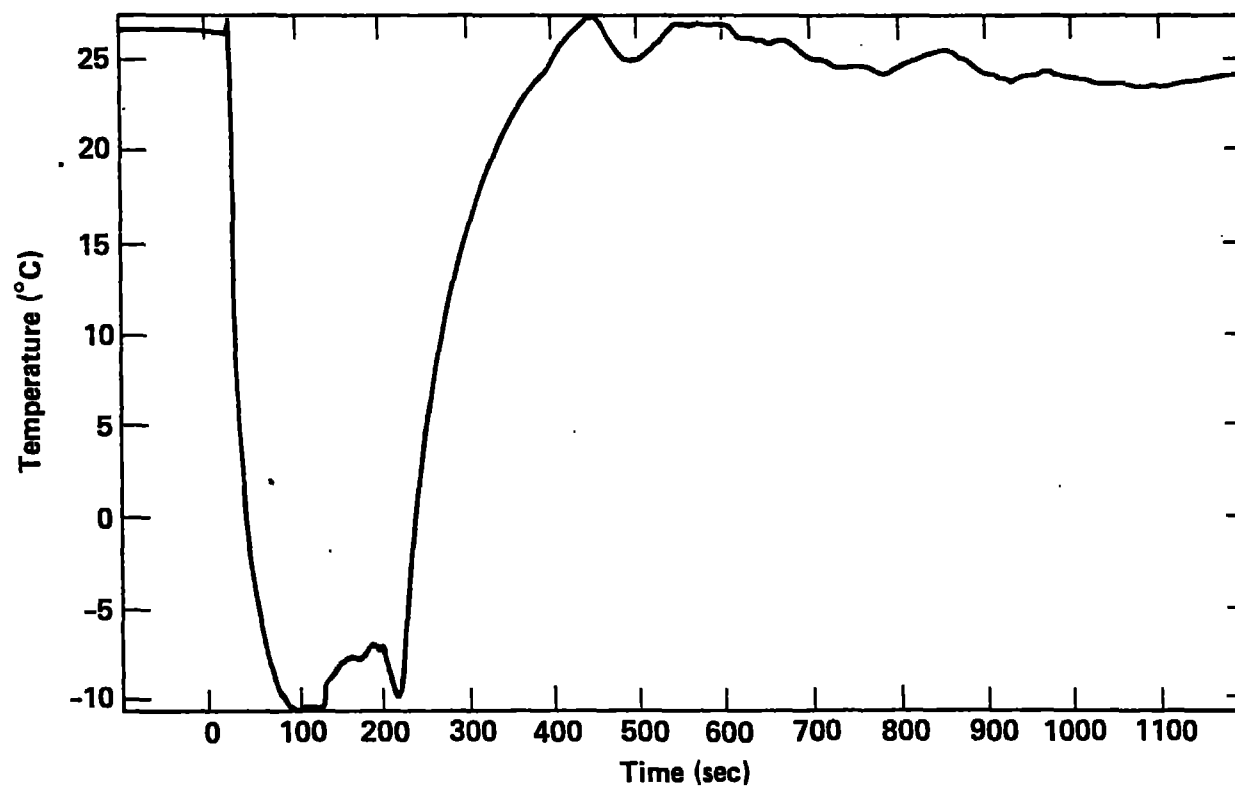


Fig. 4. Eagle 3 N_2O_4 spill area temperature data at 2 cm. above ground level.

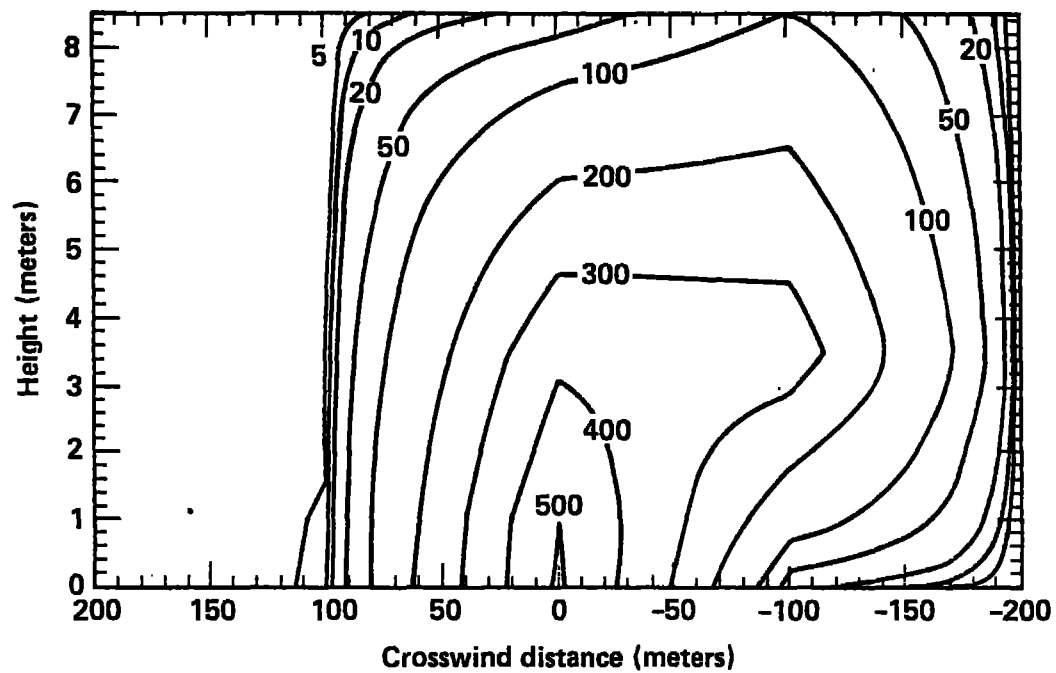
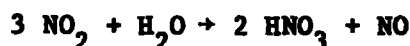


Fig. 5. Eagle 3 spill area heat flux data.

spectroscopy. None of the grab sample results indicated the presence of a foreign gas capable of producing the broad-band (4-channel) attenuation observed in the Eagle series tests. It was concluded that the attenuation must be due to aerosol scattering which does produce broad-band attenuation. Furthermore, the photography of the spills showed a definite two-phase region within the vapor cloud.

The source of the aerosol is believed to be a result of the gas-phase reaction of NO_2 with the ambient humidity, i.e.,



This reaction, and the resulting HNO_3 mist formation, has been studied in the past in regards to the scrubbing of NO_2 from exhaust stacks (Goyer, 1963; England, 1974; Peters, 1955; Chambers, 1937). The reaction is extremely fast. Experiments have shown that for typical atmospheric humidities and NO_2 concentrations greater than 50 ppm, a HNO_3 mist is instantly formed. A HNO_3 mist would also explain the severe acid damage which occurred to the instrumentation and structures in the 25 m array during the spills. Unfortunately, the IR gas sensors were not calibrated for HNO_3 mists.

The total mass spilled during Eagle 3 was 6090 kg N_2O_4 . The vapor flux results from the 25 m row of gas sensors indicate that only 1170 kg of N_2O_4 and NO_2 vapors passed through this array in the first 10 min. This is only 20% of the amount spilled. The discrepancy is due to the HNO_3 mist component and the permeation of the N_2O_4 into the ground. Although the source strength falls off dramatically after about 350 sec, this low-level soil out-gassing could continue for many hours.

The NO_2 vertical concentration contours, calculated from the gas sensor array at 785 m downwind for the Eagle 3 spill are shown in Fig. 6. The contours were calculated assuming a linear variation of the NO_2 concentration data between sensors. The maximum concentrations recorded in the 785 m array were about 50 ppm; however, this does not include the NO or HNO_3 portion of the cloud as the detectors were not sensitive to these species.

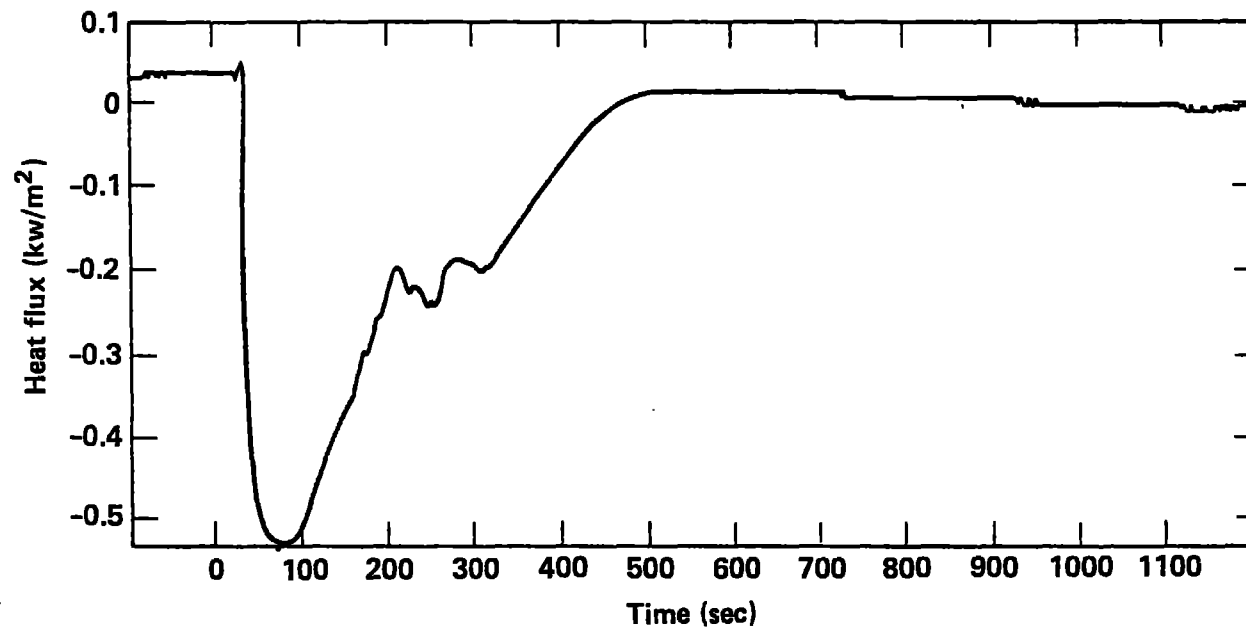


Fig. 6. Eagle 3 crosswind concentration contours at 785 m.

3.2. Preliminary NH_3 Results

The NH_3 data have not yet been reduced to final form and publicly released. Consequently, the results presented here are very preliminary and may be subject to change as data reduction continues.

The Desert Tortoise 4 test was the largest of the NH_3 series. The NH_3 was released as a horizontal jet, about 1 m above ground level, pointing downwind. The jet expanded rapidly, due to the flashing of liquid into vapor and aerosol, and was extremely turbulent. Very little liquid NH_3 pooled on the ground during the shorter tests; however, a noticeable pool was left at the end of the Desert Tortoise 4 test which lasted for nearly eight minutes. This pool represented, however, a small percentage of the total liquid spilled. Thus, most of the released NH_3 was immediately airborne either as cold vapor or aerosol. The cloud demonstrated noticeable dense gas effects, such as gravity driven slumping and spreading, as soon as the strong jetting and turbulence effects associated with the release were overcome. These source related effects were still present in the mass-flux arc of sensors at 100 m downwind but appeared from photographs to be considerably damped by the time the cloud reached twice this distance downwind. The vapor and aerosol plume, measured at the 100 m arc was considerably wider for test 4 than for the other tests. This indicates that the effects of gravity slumping and increased atmospheric stability were already important at the 100 m arc.

The maximum gas concentration as a function of downwind distance is given in Table VI for Desert Tortoise spill tests 2 through 4. The measured maximum gas concentrations from the Desert Tortoise 4 test are plotted in Fig. 7 along with predictions by the modified transient Gaussian plume model and the FEM3 model (Chan, 1983). The measured points for test 4 are the result of careful recalibration of the sensors and checking of the data and are not expected to change during the rest of the data reduction process.

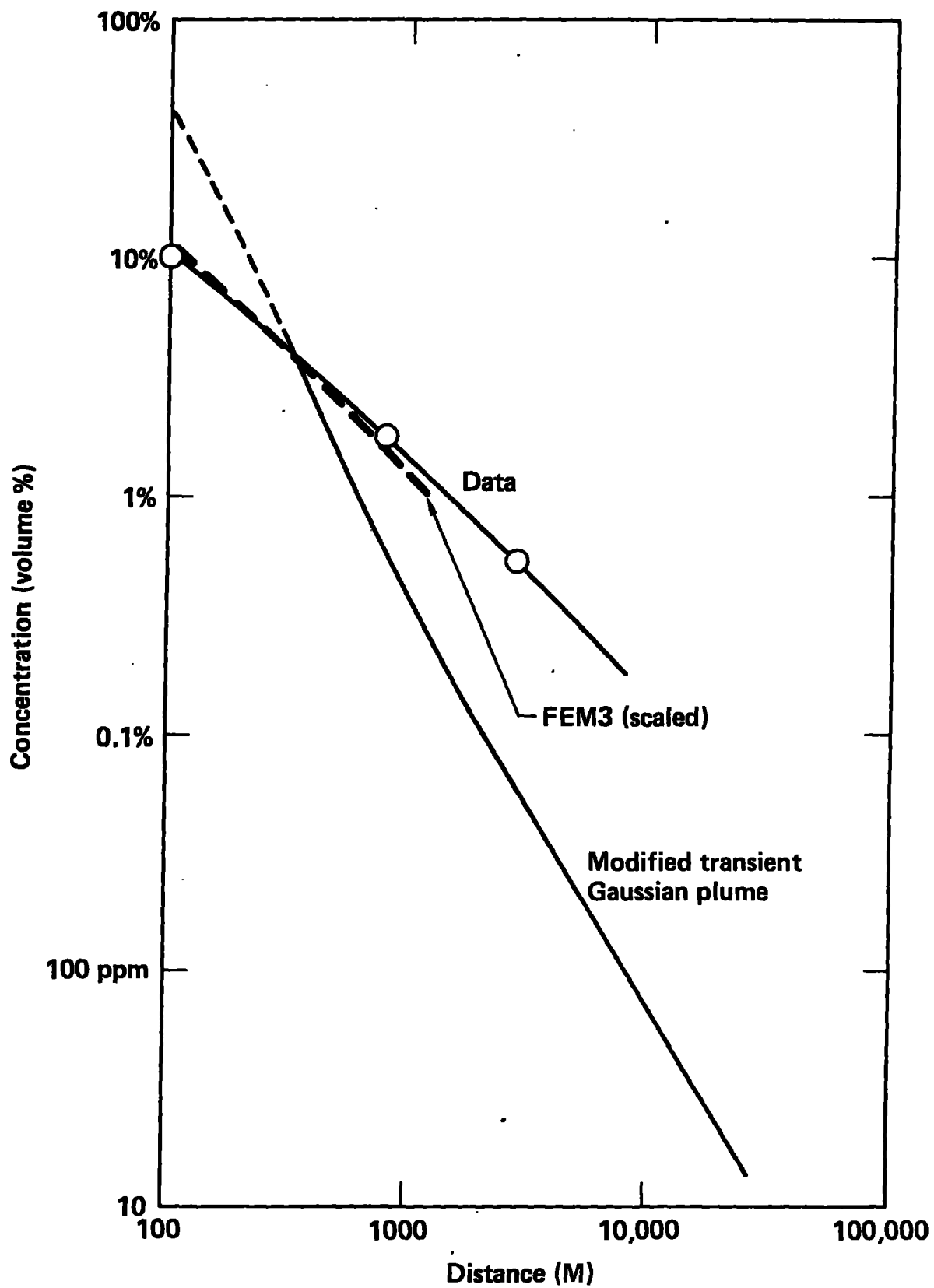


Fig. 7. Model data comparison for the Desert Tortoise 4
60 m ammonia spill.

TABLE VI. PRELIMINARY RESULTS FROM DESERT TORTOISE SERIES
 NH_3 SPILLS. MAXIMUM GAS CONCENTRATION VERSUS
 DOWNWIND DISTANCE

Test	Gas Concentration at Downwind Distance			
	100 m	800 m	1450 m	2800 m
2	9%	1.4%	> 0.5%	-
3	9%	1.6%	-	0.22%
4	10%	1.6%	-	0.53%

4. COMPARISON WITH MODEL PREDICTIONS

4.1. N_2O_4 Results Compared to the Ocean Breeze/Dry Gulch Model

The primary purpose of the Eagle test series was to demonstrate the heavy gas dispersion aspects of N_2O_4 vapors. The downwind reduction in concentration for the dispersion of a heavy gas is not as great as for a trace or neutral gas. For heavy gas dispersion, the size of the hazardous corridor can be correspondingly much greater. In late 1960, the Air Force conducted a series of dispersion tests (Haugen, 1963) at Cape Kennedy, Florida (Ocean Breeze) and at Vandenburg AFB, California (Dry Gulch). These tests involved the release and detection of a zinc sulfide tracer. There were a total of 185 tests performed under a wide range of atmospheric conditions. All of the data of the OB/DG tests were normalized and correlated to a simple diffusion prediction equation, the OB/DG model. This simple model predicted 75% of the cases to within a factor of two of the measured values.

In order to compare the results of the Eagle 3 test with the OB/DG prediction the Eagle 3 source strength must be defined. At this time, we can only place limits on source strength. We know from the heat flux data and the vapor flux calculations that the evaporation rate must certainly be greater than 23 kg/min. We also know that the maximum possible source strength must be less than the spill rate of 2030 kg/min. The results of the OB/DG concentration predictions at 785 and 2800 m for the minimum (23 kg/min) and maximum (2030 kg/min) possible Eagle 3 source strengths are given in Table VII, along with the peak measured concentrations at these locations. It appears that the

OB/DG model tends to underestimate the downwind concentration distribution of the Eagle 3 spill. The degree of the underestimate at 2800 m is not clear due to the small number of measurements and the uncertainty in source strength.

TABLE VII. COMPARISON OF EAGLE 3 NO₂ DATA AND OB/DG PREDICTIONS.

Downwind distance (m)	OB/DG Predictions (ppm)		Eagle 3 concentration measurements (ppm)
	Q = 23 kg/min	Q = 2030 kg/min	
785	7.3	630	> 500
2800	0.6	51	≥ 9*

* May not have been on cloud centerline

4.2. NH₃ Results Compared to the Modified Gaussian Plume and FEM3

The primary purpose of the NH₃ experiments was to measure the effect of aerosols on the dispersion of the NH₃ vapor. Three-dimensional hydrodynamics codes (Kansa et al., 1983; Chan, 1983) have been used successfully to predict Liquefied Natural Gas dispersion and have recently been modified to include aerosol effects for high concentrations close to the spill point. For low concentrations, long distances downwind, the Gaussian model was believed to be adequate.

It was found that the continuous (steady-state) Gaussian plume model (Hanna et al., 1982) overestimates the dispersion distances for low gas concentrations because of the short duration (4 min) of the spills. It would require a spill duration in excess of an hour for the concentration at 7-8 km to reach steady state in 2 m/sec wind. The Gaussian puff model (Hanna et al., 1982) also overestimates the dispersion distance because it assumes an instantaneous release, which is then translated downwind as a single puff.

In order to improve the estimation procedure, the Gaussian plume model was modified to account for a finite duration of release and to include the along-wind dispersion component. The transport velocity was corrected for height using a vertical power law function used by EPA (Irwin, 1979), and an

initial source geometry was assumed ($\sigma_y = 5$ m, $\sigma_z = 1$ m) corresponding to an initially heavy gas. Dispersion due to shear was determined by the method of Wilson (1981).

This modified transient Gaussian plume technique was thought to provide an adequate basis for estimating concentrations at long distances downwind where dense gas effects were believed to no longer be very important. The comparison of data from Desert Tortoise 4 and the modified transient Gaussian plume model is shown in Fig. 7. Clearly, the Gaussian calculation is inadequate. The data indicates that dense gas and aerosol effects exist well beyond the region near the spill point, to distances of at least 3 km downwind.

Since the calculation of dense gas/aerosol effects appears to be necessary for NH_3 spill predictions, a simple aerosol fog model was created for FEM3. The high-pressure release of NH_3 can result in as much as 83% of the mass of the NH_3 cloud in the liquid phase as a suspension of very fine droplets. The standard approach for treating a two-phase aerosol fog would be to add the additional partial differential equations (PDEs) for mass, momentum, and energy conservation of the liquid phase to the existing FEM3 model. In three dimensions, such an approach is computationally very expensive. Other approaches for dealing with the two-phase problem are reported in the PNL report (1981) and Kaiser and Walker, 1978.

The approach taken by Kansa et al. (1983) was to capture the essential behavior of a negatively buoyant two-phase vapor-droplet fog while using a conceptually simple model of the physics. Special physical features of the two-phase fog are the high average density of the fog, due to the liquid droplets, and the considerable amount of heat that must be added to the cloud in order to evaporate the droplets. The PDEs were solved for mass, momentum, energy, and species by assuming the aerosol fog to be a special type of vapor.

The behavior of the two-phase fog as it approaches a pure vapor cloud is modeled by means of a continuous temperature-dependent molecular weight and heat capacity. The simplifying assumptions are that the transition from liquid to vapor phase is accomplished over a temperature range, ΔT , over which the cloud is continuously transformed from a mixture of droplets (liquid phase) and vapor to pure vapor. The other assumption is that the fog behaves, over small pressure ranges, as an ideal gas. The approximations used are justified by focusing solely upon the governing physics of the dense gas dispersion, and ignoring the details of the suspension of NH_3 droplets.

A FEM3 calculation of the release of 40 tons (130 m^3) of NH_3 in 4 min. into a constant wind of 5 m/s and neutral stability conditions was performed earlier shown in Fig. 8. This calculation cannot be compared directly with the NH_3 data, but if it is scaled down, the qualitative agreement with the data, as shown in Fig. 7, is very good. The aerosol dominated dense gas effects appear to be accounted for in this type of calculation, whereas the Gaussian treatment is not adequate even for concentrations as low as 0.5% and downwind distances as great as 3 km.

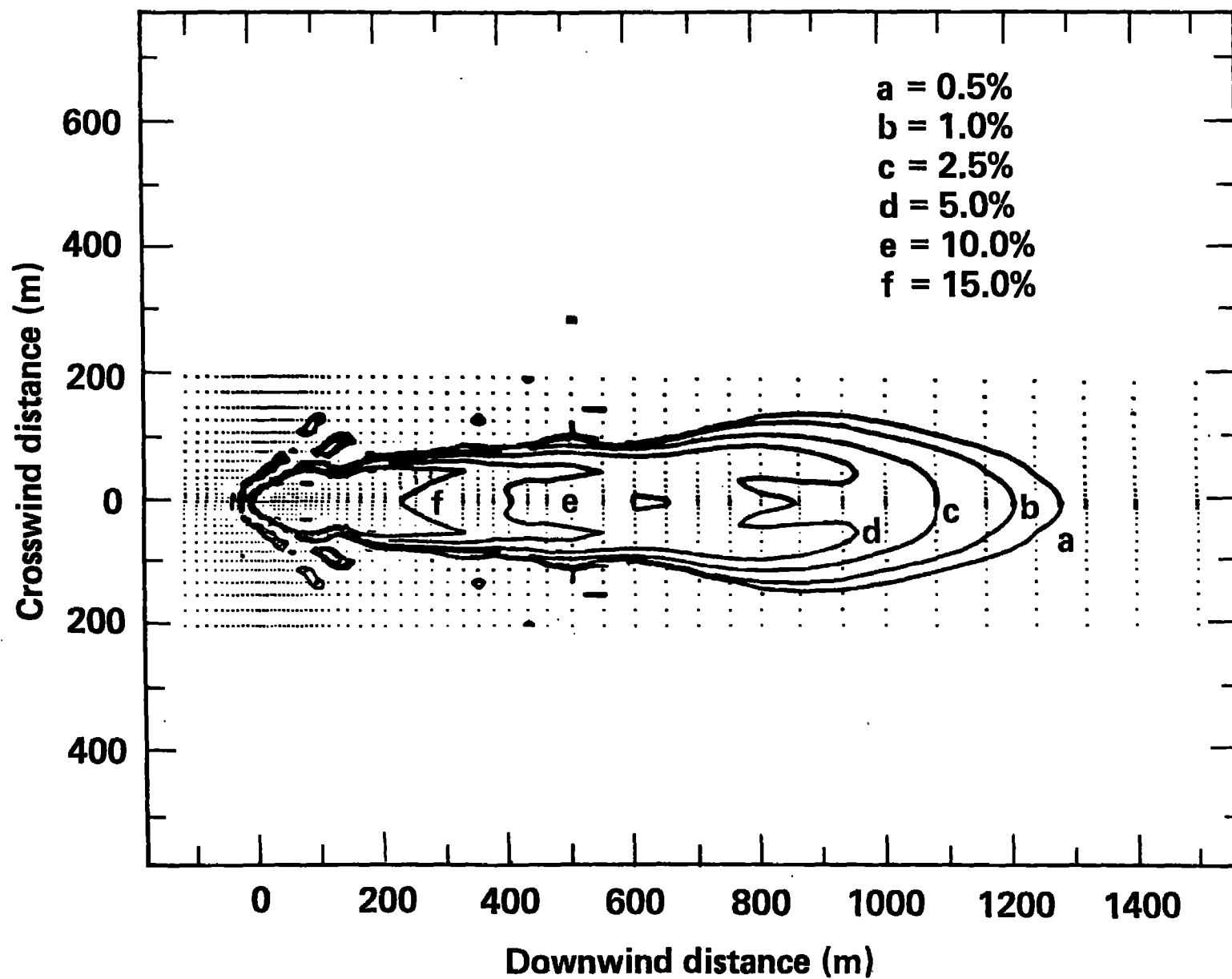


Fig. 8. Horizontal concentration contours (0.5 m above ground level) of a FEM3 plus aerosol model calculation of a 40-ton ammonia release into a 5 m/s wind and neutral stability conditions.

5. REFERENCES

- Baker, J., The LLL Data Acquisition System for the Liquefied Gaseous Fuels Program, Lawrence Livermore National Laboratory, Livermore, CA, UCID-18576, March 1980.
- Bingham, G.E., R.D. Kiefer, C.H. Gillespie, T.G. McRae, H.C. Goldwire, Jr., and R.P. Koopman, A Portable, Fast-Response Multiwavelength Infrared Sensor for Methane and Ethane in the Presence of Heavy Fog, Lawrence Livermore National Laboratory, Livermore, CA, UCRL-84850, November 1980.
- Chambers, F.S., Jr., and T.K. Sherwood, 'Absorption of Nitrogen Dioxide by Aqueous Solutions,' Ind. & Eng. Chem., 29, p. 1415 (1937).
- Chan, S.T., FEM3--A Finite Element Model for the Simulation of Heavy Gas Dispersion and Incompressible Flow: User's Manual, Lawrence Livermore National Laboratory, Livermore, CA, UCRL-53397, February 1983.
- England, C., and W.H. Corcoran, 'Kinetics and Mechanisms of the Gas-Phase Reaction of Water Vapor and Nitrogen Dioxide,' Ind. & Eng. Chem. Fundamentals, 13, p. 173 (1974).
- Goyer, G.G., 'The Formation of Nitric Acid Mists,' J. Colloid Sci., 18, p. 616-624 (1963).
- Hanna, S.R., G.A. Briggs, and R.P. Hosker, Jr. 1982. Handbook on Atmospheric Diffusion, DOE/TIC-11223, Technical Information Center, U.S. Department of Energy., 102 p.
- Haugen, D.A., and J.J. Fuguay, The Ocean Breeze and Dry Gulch Diffusion Programs, I, II, AFCRL-63-791, November, 1963.
- Irwin, J.S, 1979, A theoretical variation of the wind profile power law exponent as a function of surface roughness and stability. Atmospheric Environment, 13: 191-194.
- Kaiser, G.D., and B.C. Walker, Atmospheric Environment, 12, p. 2289-2300 (1978).
- Kansa, E.J., D.L. Ermak, S.T. Chan, and H.C. Rodean, Atmospheric Dispersion of Ammonia: An Ammonia Fog Model, Lawrence Livermore National Laboratory, Livermore, CA, UCRL-88649, January 1983; Proceedings of the Multiphase Synfuels Heat Transfer 21st ASME/AIChE National Heat Transfer Conference, Seattle, WA, July 24-28, 1983.
- McRae, T.G., R.T. Cederwall, H.C. Goldwire, Jr., D.L. Hipple, G.W. Johnson, R.P. Koopman, J.W. McClure, L.K. Morris, Eagle Series Data Report, UCID-20063, Lawrence Livermore National Laboratory, Livermore, CA, June 1984.
- Pacific Northwest Laboratory, 1981, Assessment of Research and Development Needs in Ammonia Safety and Environmental Control, PNL-4006, Pacific Northwest Laboratory, Richland, Washington.

Peters, M.S., and J.L. Holman, 'Vapor and Liquid-Phase Reactions Between Nitrogen Dioxide and Water,' Ind. & Eng. Chem., 47, p. 2536 (1955).

Wilson, D.J., 1981, Along-wind diffusion of surface transients, Atmospheric Environment, 15: 489-495.